Вестник РУДН. Серия: МЕДИЦИНА
RUDN Journal of MEDICINE. ISSN 2313-0245 (Print). ISSN 2313-0261 (Online)
2026;30(1)
http://journals.rudn.ru/medicine

DOI 10.22363/2313-0245-2025-30-1-80-91
EDN CYTWAR

ORIGINAL RESEARCH
ОРИГИНАЛЬНОЕ ИССЛЕДОВАНИЕ

Musculoaponeurotic layer structural alterations of the anterior abdominal wall in ventral hernias: insights from CT texture analysis

Andrey V. Protasov, Liya B. Kanakhina ✉, Olga I. Mazurova

RUDN University, *Moscow, Russian Federation*
✉ glb.1994@mail.ru

Abstract. *Relevance*. Postoperative ventral hernias (POVH) remain a significant surgical challenge, characterized by remodeling of the musculoaponeurotic layer of the anterior abdominal wall and loss of functional integrity. Computed tomography (CT) texture analysis enables an objective assessment of tissue microarchitecture, facilitates the identification of structural changes, and optimizes preoperative planning and surgical decision-making. *Aim*. To evaluate structural changes in the musculoaponeurotic layer of the anterior abdominal wall in healthy individuals and patients with W2 and W3 POVH using texture analysis, identify intergroup differences, and determine the topographic-anatomical characteristics of affected tissues. *Materials and Methods*. This study included 90 patients (30 without hernias, 30 with W2-POVH, 30 with W3-POVH) examined between 2020 and 2024. All patients underwent multislice computed tomography (MSCT), and axial slices were segmented using Roboflow. The resulting masks were analyzed for texture characteristics, including brightness (mean_gray), contrast (contrast), correlation (correlation), kurtosis (kurtosis_gray), skewness (skewness_gray), standard deviation (std_gray), LBP, wavelet analysis, and gabor filtering. Statistical analysis included ANOVA, the Kruskal–Wallis test, and Tukey's post-hoc analysis. *Results and Discussion*. Texture analysis revealed significant differences in Wavelet and Gabor response ($p < 0.0001$). Group 2 exhibited marked structural alterations, while Groups 1 and 3 demonstrated similar tissue characteristics ($p > 0.05$), suggesting adaptive remodeling in patients with severe hernia defects. Further, Group 2 showed significant changes in contrast ($p < 0.0001$), correlation ($p < 0.0001$), and kurtosis ($p = 0.001$), while brightness (mean_gray) and homogeneity (homogeneity) did not differ significantly ($p > 0.05$). *Conclusion*. The most pronounced structural disorganization was observed in W2-POVH patients, indicating morphofunctional instability. In contrast, W3-POVH patients exhibited adaptive changes, suggesting compensatory remodeling. These findings confirm the progressive nature of morphological changes in POVH and highlight the importance of texture analysis for personalized surgical planning.

Keywords: textural analysis, postoperative ventral hernia, musculo-aponeurotic layer, structural changes, adaptive changes, fibrosis, surgical tactics

Funding. The study was carried out without external funding.

Author contributions. A.V. Protasov, L.B. Kanakhina, O.I. Mazurova — concept and study design, O.I. Mazurova, A.V. Protasov — data collection and processing, manuscript drafting, and editing, L.B. Kanakhina, A.V. Protasov — data analysis, O.I. Mazurova, A.V. Protasov, L.B. Kanakhina — manuscript drafting, and editing.

All authors made significant contributions to the conception, conduct of the study and preparation of the article, and read and approved the final version before publication.

Consent of interest statement. All patients provided informed voluntary consent to participate in the study according to the Helsinki Declaration of the World Medical Association (WMA Declaration of Helsinki — Ethical Principles for Medical Research Involving Human Subjects, 2013) and personal data processing.

Ethics approval. The study was approved by the Ethics Committee of the Medical Institute of the RUDN University, Moscow, Russia (protocol No. 28 dated May 16, 2024).

Acknowledgements — not applicable.

Received 11.04.2025 Accepted 01.07.2025.

Consent for publication. All patients provided informed voluntary consent to participate in the study according to the Helsinki Declaration of the World Medical Association (WMA Declaration of Helsinki — Ethical Principles for Medical Research Involving Human Subjects, 2013) and personal data processing.

For citation: Protasov AV, Kanakhina LB, Mazurova OI. Musculoaponeurotic layer structural alterations of the anterior abdominal wall in ventral hernias: insights from CT texture analysis. *RUDN Journal of Medicine*. 2026;30(1):80–91. doi: 10.22363/2313-0245-2026-30-1-80-91. EDN: CYTWAR

Introduction

Postoperative ventral hernia (POVH) is a common complication following abdominal surgeries, with an incidence rate ranging from 9% to 20% within the first year postoperatively [1]. According to studies, this rate increases to 22.4% within three years after laparotomy [2]. The primary pathogenic factors contributing to the development and progression (recurrence) of POVH include degenerative changes in the postoperative scar area and the musculoaponeurotic layer of the anterior abdominal wall, particularly in patients with high-risk factors for hernia formation [3, 4].

From a biomechanical perspective, the linea alba endures the highest mechanical loads in patients with postoperative ventral hernias [3]. Consequently, deformation of the linea alba results in unbalanced lateral forces due to intra-abdominal pressure and involuntary contractions of the oblique and transverse muscles, leading to their retraction and shortening. This muscle shortening may cause irreversible contractures or reversible spasticity, further contributing to the lateral displacement of the rectus abdominis muscles, hernia formation, and its progression.

Prolonged herniation, especially in large and giant hernias, leads to remodeling of the abdominal wall muscles. Chronic exposure to pathological protrusion results in muscle atrophy, excessive fibrosis, and microcirculatory disturbances [5]. These changes are associated with a loss of muscle elasticity and strength, complicating surgical treatment and increasing the risk of recurrence. However, depending on the defect size and the extent of tissue involvement, the morphological and functional changes in the anterior abdominal wall may vary significantly. Preoperative assessment of the musculoaponeurotic layer remains a complex task, as conventional imaging techniques do not always allow for quantitative evaluation of structural alterations.

Modern approaches to medical image analysis include texture analysis, which enables the detection of subtle changes in tissue structure by assessing its heterogeneity, density, and spatial organization.

Computed tomography (CT) is an X-ray-based imaging modality that registers the attenuation of X-ray radiation as it passes through biological tissues. CT images are generated due to variations in the linear attenuation coefficient (μ), which is determined by the tissue's composition and density. The primary

quantitative parameter used in CT imaging is the Hounsfield Unit (HU, Hounsfield Units), calculated using the following equation [6]:

$$HU = 1000 \times \frac{\mu - \mu_{\text{water}}}{\mu_{\text{water}} - \mu_{\text{air}}}$$

where μ_{water} — is the attenuation coefficient of water, a μ_{air} — is the attenuation coefficient of air, μ — represents the attenuation coefficient of the tissue.

Each tissue type has a specific range of Hounsfield Units (HU): air (≈ –1000 HU), fat (≈ –100 HU), soft tissues (0–80 HU), and bones (700–3000 HU). Thus, the grayscale intensity in CT imaging is directly correlated with the radiological density of tissues and their atomic composition.

Traditional visual analysis of CT slices is limited by subjective interpretation in disease diagnostics, whereas quantitative methods, such as texture analysis, enable a detailed assessment of tissue heterogeneity.

Traditional diagnostic approaches, including visual assessment, morphometry, and manual classification, remain fundamental tools in medical imaging. Visual interpretation of images, based on subjective evaluation of grayscale gradients and anatomical structures, is widely used in clinical practice. However, this approach is characterized by a high degree of subjectivity, influenced by the individual perception of the physician, which can lead to variability in diagnostic outcomes. Additionally, the sensitivity of visual analysis is limited, making it challenging to detect subtle structural changes, while the absence of quantitative parameters prevents standardization in diagnostics.

Morphometry, as a method of quantitative assessment of anatomical structures, involves measuring their size, shape, and volume. In medical practice, morphometric parameters such as tissue thickness, pathological volume, and degree of deformation are used for disease diagnosis and prognosis. However, this method is limited by its inability to account for histological tissue heterogeneity, making it insufficient for a comprehensive characterization of structural changes. Furthermore, morphometric analysis requires significant time investment and manual data processing, reducing its efficiency in routine clinical applications.

The application of texture analysis in CT imaging allows for a quantitative assessment of tissue heterogeneity, revealing structural patterns that are not detectable through conventional diagnostic methods. Unlike visual analysis and morphometry, texture analysis relies on numerical parameters, eliminating subjective bias and improving reproducibility. This method exhibits high sensitivity to microscopic structural alterations and enables multiparametric analysis, including the evaluation of contrast, homogeneity, correlation, and other characteristics. Automating data processing significantly accelerates diagnosis and facilitates large-scale data analysis, which is particularly critical for personalized treatment planning. Thus, the integration of texture analysis into clinical practice enhances medical imaging capabilities by providing a standardized, reproducible, and precise method for diagnosing structural tissue changes.

Texture analysis is based on mathematical modeling of the spatial distribution of pixel intensities and enables the computation of parameters such as contrast, correlation, homogeneity, entropy, and other statistical features [7, 8].

One of the most widely used methods is the Gray-Level Co-occurrence Matrix (GLCM), which models the probability of pairs of pixels with specific grayscale values occurring at a fixed spatial distance from each other [9]. The key parameters of GLCM include: contrast, which characterizes the degree of difference between neighboring pixels and is calculated using the formula:

$$\text{Contrast} = \sum_{i=0}^{N-1}\sum_{j=0}^{N-1} P(i,j)(i-j)^2$$

Correlation, which measures the linear dependence between grayscale levels and is calculated using the formula:

$$Correlation = \sum_{i=0}^{N-1}\sum_{j=0}^{N-1} P(i,j)\frac{(i-\mu_i)(j-\mu_j)}{\sigma_i\sigma_j}$$

where μ_j are the mean grayscale values, and σ_i and $\sigma_j$are the standard deviations of grayscale levels in the image. Homogeneity, which evaluates the degree of texture smoothness and is calculated using the formula:

$$\text{Homogeneity} = \sum_{i=0}^{N-1}\sum_{j=0}^{N-1}\frac{P(i,j)}{1+(i-j)^2}$$

This parameter measures how uniform the distribution of grayscale intensities is, assigning higher values to images with low contrast and smooth transitions between pixel intensities.

The Local Binary Patterns (LBP) method analyzes the microtexture of an image by encoding differences between the central pixel and its neighboring pixels into a binary code. First introduced by Ojala et al., LBP is a powerful tool for microtexture analysis [10]. It is based on comparing the intensity of the central pixel with its surrounding pixels and generating a binary code that reflects local variations in brightness.Formally, LBP is defined as follows:

$$LBP = \sum_{p-0}^{P-1} s\,(I_P - I_c)\times 2^p, s(x) = \begin{cases}1, x \geq 0\\ 0, x < 0\end{cases}$$

where I_c — the intensity of the central pixel, I_P — represents the intensities of the neighboring pixels, P — number of neighbors, $s(x)$ is a step function that assigns binary values based on the difference in intensity.

The LBP method enables texture classification based on local gradient variations, making it a valuable tool for analyzing medical images, including oncological diagnostics, the assessment of structural tissue changes, and the identification of pathological features in histological specimens.

Wavelet analysis is a multi-scale image processing technique that decomposes texture into components with different spatial-frequency characteristics [11, 12]. Unlike the traditional Fast Fourier Transform (FFT), which analyzes an image in a fixed frequency domain, Wavelet transformation provides simultaneous localization in both space and frequency, allowing for a more detailed characterization of structural patterns. Mathematically, the Wavelet decomposition of a signal is defined as the convolution of the original image f(*x*, *y*) with a basis function ψ(*x*, *y*):

$$W(x,y,s) = \\ = \int\int f(x',y')\psi*(sx'-x, sy'-y)dx'dy'$$

where s — denotes the scale parameter, which controls the level of decomposition, $\psi(x,y)$ — represents the scaled and translated wavelet function

The application of Wavelet Energy allows for the assessment of texture energy distribution across different frequency ranges, making this method particularly useful for analyzing soft tissue structures, identifying anomalies, and predicting pathological changes [13, 14].

Gabor filters are directional filters that enable the analysis of periodic structures and spatial-frequency characteristics of an image [15]. They model the spatial-frequency sensitivity of visual cortex receptors and are widely used in texture analysis for extracting distinctive image features. The two-dimensional Gabor function is defined by the following equation:

$$G(x,y,\lambda,\theta,\psi,\sigma,\gamma) = \\ = \overline{\exp}\left(-\frac{x'^2+\gamma^2y'^2}{2\delta^2}\right)\cos\left(2\pi\frac{x'}{\lambda}+\psi\right)$$

where $\boldsymbol{x'=x\cos\theta+y\sin\theta}$, $\boldsymbol{y'=-x\sin\theta+y\cos\theta}$, $\boldsymbol{\lambda}$ (wavelength) controls the spatial frequency of the filter, **θ** (orientation) defines the direction of the filter, **σ** (scale) determines the standard deviation of the Gaussian envelope, **γ** (aspect ratio) adjusts the ellipticity of the Gaussian function, **ϕ** (phase offset) shifts the cosine function.

In addition to the Gray-Level Co-occurrence Matrix (GLCM), texture analysis of medical images utilizes statistical parameters that characterize the distribution of pixel intensities. One of the key metrics is the mean gray level (mean_gray), which represents the average intensity of pixels and reflects the density of the examined tissue. Another essential parameter is the standard deviation of the gray level (std_gray), which quantifies the variability of intensity values, allowing

for an objective assessment of structural heterogeneity in the image.

To analyze the shape of the intensity distribution, the skewness (skewness_gray) metric is used, which indicates the asymmetry of the distribution relative to the mean intensity. Negative skewness suggests the presence of predominantly darker regions, whereas positive skewness indicates the dominance of brighter areas. Another critical metric is kurtosis (kurtosis_gray), which reflects the "sharpness" of the intensity distribution and is particularly useful for detecting outliers and anomalous pixel values, making it especially important for evaluating heterogeneous structures.

The application of these statistical characteristics in CT texture analysis enables a detailed assessment of tissue microarchitecture, identification of deviations from normal structure, and classification of pathological changes. Texture analysis not only reveals the morphological features of tissues but also provides a quantitative assessment of their alterations, making it a promising tool in the diagnosis of various pathologies.

The use of Wavelet analysis, Gabor filtering, and Local Binary Patterns (LBP) for evaluating the textural characteristics of the musculoaponeurotic layer of the anterior abdominal wall offers greater precision in differentiating tissue conditions in patients with ventral hernias [16, 17].

Modern quantitative CT image analysis techniques continue to evolve, providing new opportunities for objective assessment of anatomical structures and pathological alterations. Beyond classical texture analysis — comprising methods such as GLCM, LBP, Wavelet analysis, and Gabor filtering — deep neural networks, machine learning, and radiomics have gained significant attention. These advanced techniques allow for a more detailed analysis of medical images by automatically extracting features and incorporating them into predictive models.

Deep learning is a powerful tool for medical image processing, enabling automatic segmentation, classification, and pathology detection. The foundation of these methods lies in convolutional neural networks (CNNs), which can extract relevant features without the need for manual selection of textural characteristics [18].

The architecture of Convolutional Neural Networks (CNNs) consists of several key components:

- Convolutional layers, which apply filters to input images and extract texture-based features.
- Pooling layers, which reduce the dimensionality of the feature space and enhance robustness to spatial shifts.
- Fully connected layers, which are used for classification or regression based on the extracted features.

One of the most effective architectures for medical imaging is U-Net [19]. This neural network model is specifically designed for image segmentation and is widely applied in radiology. Unlike traditional segmentation algorithms, U-Net employs an encoder-decoder strategy, allowing it to capture both local and global image features simultaneously.

Deep neural networks are also utilized in automated pathology detection, including the recognition of tumors, fibrosis, and degenerative tissue changes [20]. However, the primary limitations of this approach include high computational complexity, the need for large annotated datasets, and limited model interpretability.

In addition to neural network-based approaches, classical machine learning algorithms play a significant role in CT image analysis. Techniques such as gradient boosting (XGBoost, LightGBM), random forests (Random Forest), and support vector machines (SVM) [21] enable the development of predictive models based on quantitative image features, including textural, morphometric, and intensity-based parameters.

A key advantage of machine learning algorithms is their ability to combine diverse datasets and efficiently operate on relatively small sample sizes. For instance, the random forest method constructs ensembles of decision trees, reducing overfitting risk and enhancing model stability. Meanwhile, gradient boosting demonstrates high accuracy in classification and regression tasks by sequentially training weak models and integrating them into a unified system.

Radiomics is a methodology for multiparametric image analysis, involving the extraction and quantitative assessment of textural, morphometric, and spatial features. This approach enables the identification of hidden patterns that are inaccessible through traditional

visual analysis or even through individual machine learning techniques [22].

The radiomics pipeline consists of several key stages:

- Image segmentation, identifying the region of interest (ROI).
- Feature extraction, including textural characteristics, shape descriptors, and intensity metrics.
- Data filtering, removing non-informative parameters.

Model development, creating predictive models using machine learning techniques.

One of the primary advantages of radiomics is its potential for personalized diagnostics and prognostic analysis. In oncology, this method is widely applied for tumor aggressiveness assessment, therapy response prediction, and patient risk stratification [23]. By analyzing the textural characteristics of tumor formations, it is possible to identify radiomic signatures that correlate with molecular tumor features and clinical outcomes.

Deep learning, machine learning, and radiomics represent promising approaches for quantitative CT image analysis, expanding the capabilities of traditional visual assessment and textural feature extraction. Deep learning enables the automatic extraction of meaningful features, machine learning facilitates predictive modeling based on textural parameters, and radiomics integrates a broad spectrum of quantitative image characteristics.

Despite their high accuracy, the clinical implementation of these methods requires standardization, validation, and the development of reproducible data processing protocols. Further research on the integration of AI-driven approaches will contribute to enhancing diagnostic accuracy and improving the personalization of medical decision-making.

Aim

The objective of this study was to assess structural changes in the musculoaponeurotic layer of the anterior abdominal wall in healthy patients and those with ventral hernias of W2 and W3 categories using texture analysis of CT images. The study aims to identify quantitative and qualitative differences between groups based on key textural parameters and to evaluate the nature of structural tissue changes depending on the stage of the pathological process.

Materials and methods

This study was conducted at the Federal State Budgetary Healthcare Institution Clinical Hospital No. 85 of the Federal Medical and Biological Agency of Russia and the Private Healthcare Institution "Clinical Hospital RZD-Medicine" named after N.A. Semashko. The dataset included 90 patients who underwent examination or treatment between January 2020 and September 2024. All patients provided informed voluntary consent to participate in the study according to the Helsinki Declaration of the World Medical Association (WMA Declaration of Helsinki — Ethical Principles for Medical Research Involving Human Subjects, 2013) and personal data processing. The study was approved by the Ethics Committee of the Medical Institute of the RUDN University, Moscow, Russia (protocol No. 28 dated May 16, 2024).

For analysis, three independent groups were formed: group 1 (N=30): patients without postoperative ventral hernias (POVH) who were examined or treated for unrelated chronic pathology. Group 2 (N=30): patients diagnosed with W2 POVH. Group 3 (N=30): patients with large or giant ventral hernias (W3), who were candidates for preoperative botulinum therapy before surgical intervention.

All patients underwent computed tomography (CT) of the thoracic cavity, abdominal cavity, and pelvic organs (three anatomical regions) (Figure 1).

In the axial CT series, segmentation of the anterior abdominal wall muscles was performed, including the external oblique muscle (m. obliquus externus abdominis), internal oblique muscle (m. obliquus internus abdominis), and transverse abdominal muscle (m. transversus abdominis) on both the right and left sides. The segmentation of anatomical structures was carried out using the Roboflow platform (https://app.roboflow.com) through automated segmentation methods with manual correction when necessary. The U-Net convolutional neural network was used as the baseline algorithm for segmentation (Figure 2).

Fig. 1. Example of a CT series in the axial projection for segmentation

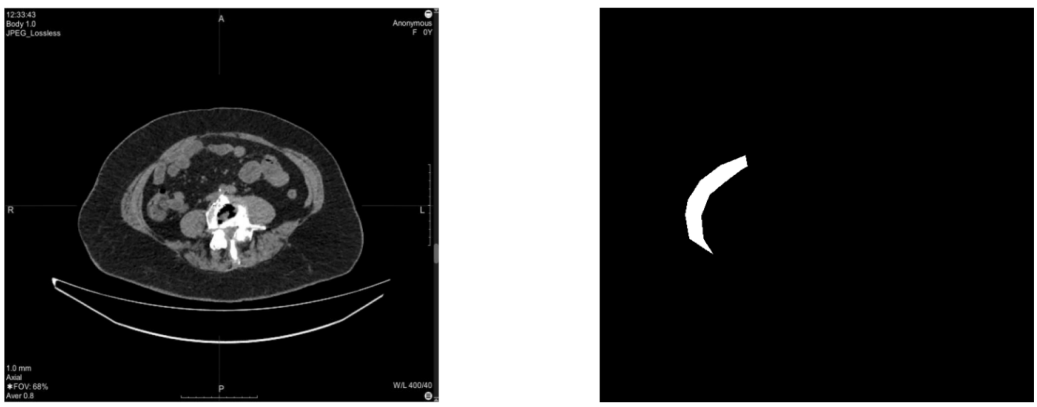

Fig. 2. An example of a CT scan and the corresponding mask of the musculo–aponeurotic layer of the anterior abdominal wall on the right

To enhance the accuracy of annotation, manual correction of segmentation masks was performed following automated segmentation, allowing for the minimization of errors associated with tissue heterogeneity and intensity gradient variability.

For the correct analysis of CT image texture characteristics, preprocessing was applied, including pixel intensity normalization, artifact suppression, and contrast optimization. Normalization was performed using intensity standardization, following the formula:

$$I' = \frac{I - \mu}{\delta}$$

where: I' — is the normalized intensity, I — the original pixel intensity, μ — the mean intensity of the image, δ — the standard deviation of intensity values.

This procedure minimized variability in scanning conditions and standardized gray-level intensity across all images. To eliminate artifacts caused by noise, metallic objects, and tissue density variations, a Gaussian filter and bilateral filtering were applied.

Contrast enhancement was performed using histogram equalization, which redistributes gray-level intensities based on their cumulative distribution. The integration of a comprehensive preprocessing approach, including normalization, artifact suppression, and automated segmentation, ensured standardization of CT images and improved the reproducibility of subsequent texture analysis.

For data processing and analysis, statistical methods, machine learning techniques, and visualization tools were employed. Descriptive statistics included the computation of mean values, standard deviations, and parameter distribution analysis within each group.

Texture analysis was conducted across the three patient groups, evaluating parameters such as mean gray level (mean_gray), contrast, homogeneity, correlation, kurtosis (kurtosis_gray), skewness (skewness_gray), standard deviation of gray levels (std_gray), Local Binary Patterns (LBP), lbp_mean, and lbp_var. The analysis utilized LBP, wavelet transform, and Gabor filtering.

To assess group differences, analysis of variance (ANOVA) and the nonparametric Kruskal–Wallis test were applied, enabling the identification of statistically significant differences. In cases where significant differences were detected, post-hoc Tukey's test was performed for multiple group comparisons.

All computations and visualizations were conducted using Python 3.11 libraries, including NumPy, SciPy, scikit-learn, Matplotlib, and Seaborn.

Results and discussion

The gray density (brightness) analysis of the segmentation masks revealed that Group 1 exhibited the brightest masks (right_mean_gray = 116.41, left_mean_gray = 117.82), which may indicate lower tissue density (Figure 3).

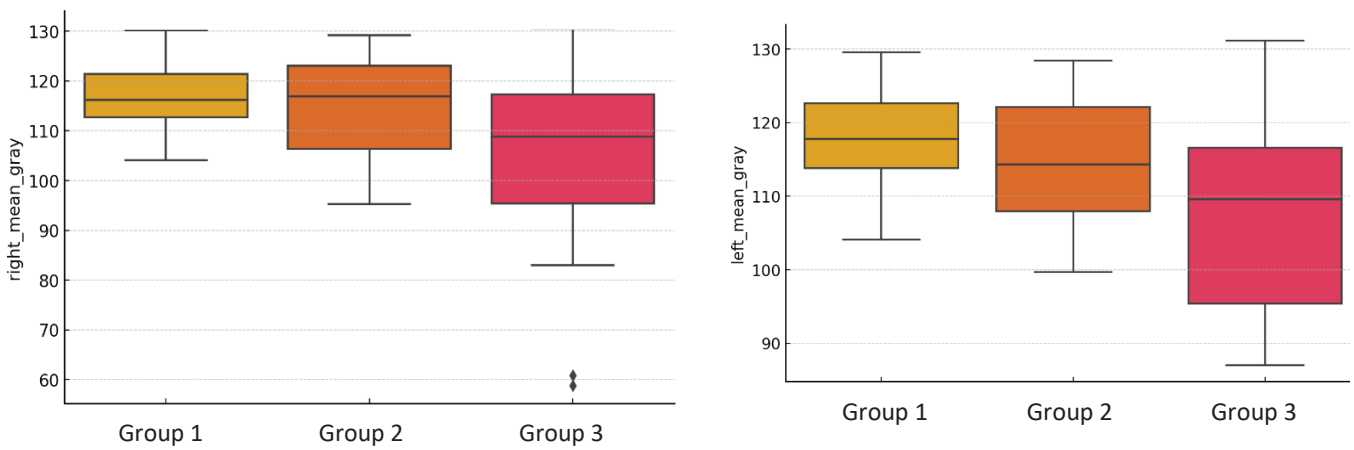

a *b*

Fig. 3. The density of gray in masks between groups (*a* and *b*). Kruskal–Wallis test with post-hoc Tukey's test, **p* < 0.05 considered significant

Group 3 exhibited the darkest masks (right_mean_gray = 106.46, left_mean_gray = 107.82), suggesting a potential increase in tissue density or the presence of fibrotic changes. Group 2 demonstrated intermediate values (right_mean_gray = 115.14, left_mean_gray = 114.89), reflecting a transitional nature of structural alterations in the musculoaponeurotic layer of the anterior abdominal wall (Figure 4).

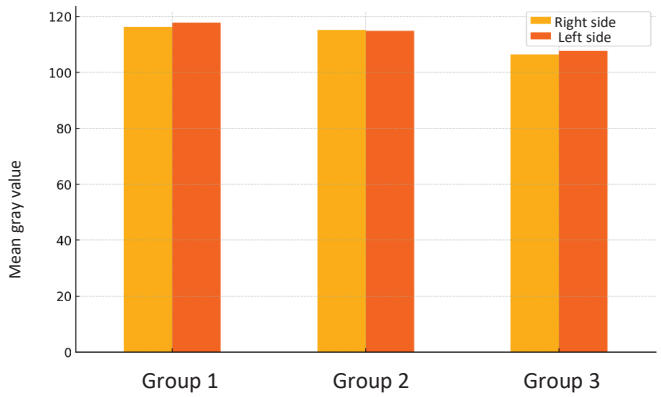

Fig. 4. Graph of gray level distribution (gray density in masks) by groups

Descriptive statistics revealed differences between groups in several key characteristics, as confirmed by analysis of variance (ANOVA) and the Kruskal–Wallis test. Statistically significant differences ($p < 0.05$) were observed for contrast and correlation on both the right and left sides, specifically: right_contrast ($p < 0.0001$), right_correlation ($p < 0.0001$), right_homogeneity ($p < 0.001$), left_contrast ($p < 0.0001$), and left_correlation ($p < 0.0001$). At the same time, features such as right_energy, right_lbp_mean, left_energy, and left_lbp_mean did not exhibit significant differences between groups, suggesting the similarity of these parameters across different clinical categories. Texture analysis demonstrated that the Wavelet Energy metric differed significantly between groups (ANOVA: $p < 0.0001$, Kruskal–Wallis test: $p < 0.0001$) (Figure 5).

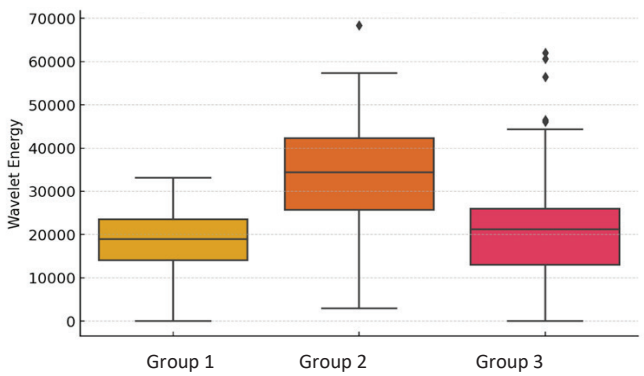

Fig. 5. Wavelet Energy indicator between groups. ANOVA: *$p < 0.0001$, Kruskal–Wallis test: * $p < 0.0001$

Post-hoc Tukey's test confirmed significant differences between Groups 1 and 2 ($p < 0.0001$) as well as between Groups 2 and 3 ($p < 0.0001$). However, no statistically significant differences were observed between Groups 1 and 3 ($p = 0.3279$), indicating that the muscle structure in Group W3 (Group 3) is more similar to normal tissue (Group 1) than to Group 2 (W2). The Gabor filtering method also identified significant differences between the groups (ANOVA: $p < 0.0001$, Kruskal–Wallis test: $p < 0.0001$) (Figure 6).

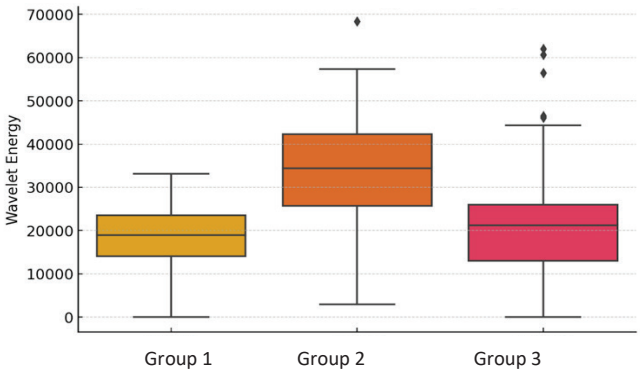

Fig. 6. Gabor filtering indicator between groups. Statistical analysis: ANOVA and Kruskal–Wallis test; *$p < 0.0001$ considered significant

Statistically significant differences were observed between Groups 1 and 2 ($p < 0.0001$), whereas differences between Groups 1 and 3 did not reach statistical significance ($p = 0.0801$). These findings suggest a trend toward normalization of muscle structure in Group 3.

Comparison of the right and left sides within each group revealed significant differences in Group 3 for the contrast parameter ($p = 0.00015$), which may indicate asymmetrical tissue changes. In Group 1, a significant difference was observed for correlation ($p = 0.033$), reflecting structural muscle characteristics. In Group 2, no statistically significant differences between sides were detected ($p > 0.05$), indicating symmetrical tissue properties in this group.

The results confirm that different stages of ventral hernias are associated with distinct types of changes in

the musculoaponeurotic layer of the anterior abdominal wall. Our findings are consistent with the results reported by Parshikov V.V. et al. [24], who demonstrated that the anatomical structure of the musculoaponeurotic layer undergoes significant alterations in ventral hernias, including changes in tissue density, fibrosis, and muscle remodeling.

Furthermore, it is well established that the use of botulinum toxin in preoperative preparation is based on the phenomenon of muscle contracture, which is particularly pronounced in W3 hernias [25]. The results of our study also support this finding, showing increased tissue density and reduced elasticity in W3 patients, which necessitates preoperative muscle relaxation for successful surgical treatment.

Thus, the observed structural changes complement existing scientific data on the mechanisms of ventral hernia formation and may contribute to the optimization of treatment strategies. Texture analysis of CT images provides an objective, quantitative assessment of pathological changes, making it a valuable tool for diagnostics and surgical decision-making. However, further research is required to evaluate the prognostic significance of the identified textural characteristics and their impact on surgical outcomes.

Conclusion

According to the obtained data, Group 1 (healthy patients) exhibits the most homogeneous muscle tissue structure, with the least changes in contrast and correlation, confirming their functional integrity and absence of pathological alterations. Group 2 (W2) demonstrates the most pronounced structural muscle changes, characterized by decreased contrast, altered pixel correlation values, and modified texture parameters, as identified through Wavelet analysis and Gabor filtering. The darkest segmentation masks were observed in Group 3, suggesting hypertrophic or compensatory changes in W3 patients, whereas tissues in W2 patients appear to be in a state of dysfunction and instability.

In terms of textural characteristics, Group 3 (W3) is closer to healthy patients (Group 1) than to Group 2, suggesting the presence of compensatory mechanisms in muscle tissue under conditions of long-standing hernias. This hypothesis is supported by the stable and homogeneously increased muscle density, along with similarity in the distribution of textural parameters between Group 3 and the control group.

References / Список литературы

1. Le Huu Nho R, Mege D, Ouaïssi M, Sielezneff I, Sastre B. Incidence and prevention of ventral incisional hernia. *J Vasc Surg*. 2012;149: e3-e14. doi:10.1016/j.jviscsurg.2012.05.004
2. Fink C, Baumann P, Wente MN, Knebel P, Bruckner T, Ulrich A, Werner J, Büchler MW, Diener MK. Incisional hernia rate 3 years after midline laparotomy. *Br J Surg*. 2014;101:51–54. doi:10.1002/bjs.9364
3. Hernández-Gascón B, Mena A, Peña E, Pascual G, Bellón JM, Calvo B. Understanding the passive mechanical behavior of the human abdominal wall. *Ann Biomed Eng*. 2013;41(2):433–444. doi:10.1007/s10439–12–0672–7
4. Deerenberg EB, Henriksen NA, Antoniou GA, Antoniou SA, Bramer W.M., Fischer JP, Fortelny RH, Gök H, Harris HW, Hope W, Horne CM, Jensen TK, Köckerling F, Kretschmer A, López-Cano M, Malcher F, Shao JM, Slieker JC, de Smet GHJ, Stabilini C, Torkington J, Muysoms FE. Updated guideline for closure of abdominal wall incisions from the European and American Hernia Societies. *Br J Surg*. 2022;109(12):1239–1250. doi:10.1093/bjs/znac302
5. Farmer SE, James M. Contractures in orthopaedic and neurological conditions: a review of causes and treatment. *Disabil Rehabil*. 2001;13:549–558. doi:10.1080/09638280010029930
6. International Atomic Energy Agency. Diagnostic Radiology Physics. Vienna: IAEA; 2014, 210 p.
7. Gonzalez RC, Woods RE. Digital Image Processing. 3rd ed. Prentice Hall; 2008. ISBN: 978–0131687288
8. Sonka M, Hlavac V, Boyle R. Image Processing, Analysis, and Machine Vision. 4th ed. Cengage Learning; 2014, 325 p.
9. Haralick RM, Shanmugam K, Dinstein I. Textural features for image classification. *IEEE Trans Syst Man Cybern*. 1973; SMC-3(6):610–621. doi:10.1109/TSMC.1973.4309314
10. Ojala T, Pietikäinen M, Harwood D. A comparative study of texture measures with classification based on featured distributions. *Pattern Recognit*. 1996;29(1):51–59. doi:10.1016/0031–3203 (95) 00067-4
11. Jain AK, Farrokhnia F. Unsupervised texture segmentation using Gabor filters. *Pattern Recognit*. 1991;24(12):1167–1186. doi:10.1016/0031-3203(91)90143-S
12. Mallat S. A theory for multiresolution signal decomposition: the wavelet representation. *IEEE Trans Pattern Anal Mach Intell*. 1989;11(7):674–693. doi:10.1109/34.192463
13. Daubechies I. Ten Lectures on Wavelets. SIAM; 1992. ISBN: 978-0-89871-274-2
14. Unser M. Texture classification and segmentation using wavelet frames. *IEEE Trans Image Process*. 1995;4(11):1549–1560.
15. Daugman JG. Uncertainty relation for resolution in space, spatial frequency, and orientation optimized by two-dimensional visual cortical filters. *J Opt Soc Am A*. 1985;2(7):1160–1169. doi:10.1364/JOSAA.2.001160
16. Sonawane MR, Agrawal DG. Texture classification with feature analysis using wavelet approach: a review. *Int J Sci Res*. 2015;4(5):433–444. [cited 2025 Feb 20]. Available from: https://www.ijsr.net/archive/v4i5/SUB154186.pdf
17. Barina D. Gabor wavelets in image processing. *arXiv preprint*. 2016;(1602.03308). [cited 2025 Feb 20]. Available from: https://arxiv.org/abs/1602.03308

18. LeCun Y, Bengio Y, Hinton G. Deep learning. *Nature*. 2015;521(7553):436–444

19. Ronneberger O, Fischer P, Brox T. U-Net: convolutional networks for biomedical image segmentation. *MICCAI*. 2015;234–241.

20. Lakhani P, Sundaram B. Deep learning at chest radiography: automated classification of pulmonary tuberculosis by using convolutional neural networks. *Radiology*. 2017;284(2):574–582. doi:10.1148/radiol.2017162326

21. Breiman L. Random forests. *Mach Learn*. 2001;45(1):5–32.

22. Lambin P., Rios-Velazquez E., Leijenaar R., Carvalho S., van Stiphout R.G.P.M., Granton P., Zegers C.M.L., Gillies R., Boellaard R., Dekker A., Aerts H.J.W.L. Radiomics: extracting more information from medical images using advanced feature analysis. *Eur J Cancer*. 2017;48(4):441–446

23. Aerts HJWL, Velazquez ER, Leijenaar RTH, Parmar C, Grossmann P, Carvalho S, Bussink J, Monshouwer R, Haibe-Kains B, Rietveld D, Hoebers F, Rietbergen MM, Leemans CR, Dekker A, Quackenbush J, Gillies RJ, Lambin P. Decoding tumour phenotype by noninvasive imaging using a quantitative radiomics approach. *Nat Commun*. 2014;5:4006

24. Parshikov VV, Loginov VI. Components separation technique in treatment of patients with ventral and incisional hernias (review). *Mod Technol Med*. 2016;8(1):183. doi:10.17691/stm2016.8.1.24

25. Whitehead-Clarke T, Windsor A. The use of botulinum toxin in complex hernia surgery: achieving a sense of closure. *Front Surg*. 2021;8:753889. doi:10.3389/fsurg.2021.753889

Структурные изменения мышечно-апоневротического слоя передней брюшной стенки при вентральных грыжах: данные текстурного анализа КТ

А.В. Протасов, Л.Б. Канахина ✉, О.И. Мазурова

Российский университет дружбы народов, *г. Москва, Российская Федерация*
✉ glb.1994@mail.ru

Аннотация. *Актуальность.* Послеоперационные вентральные грыжи (ПОВГ) представляют собой серьезную хирургическую проблему, характеризующейся ремоделированием мышечно-апоневротического слоя передней брюшной стенки и потере его функциональной целостности. Применение текстурного анализа в КТ позволит объективно оценить микроархитектонику тканей, выявить структурные изменения и оптимизировать предоперационное планирование и тактику хирургического лечения. Цель — оценить структурные изменения мышечно-апоневротического слоя передней брюшной стенки у здоровых пациентов и пациентов с W2 и W3 — ПОВГ с помощью текстурного анализа, выявить межгрупповые различия и особенности топографо-анатомической организации тканей. Материалы и методы. В ретроспективное исследование включены 90 пациентов (30 без грыж, 30 с W2-ПОВГ, 30 с W3-ПОВГ), обследованных в 2020–2024 гг. Всем пациентам выполнено МСКТ брюшной полости. Далее аксиальные срезы были сегментированы на онлайн-платформе Roboflow. Полученные маски анализировались по текстурным характеристикам: яркость, контрастность, корреляция, куртоз, асимметрия, стандартное отклонение, LBP, вейвлет- и Габор-анализ. Для статистической обработки использованы ANOVA, критерий Крускала–Уоллиса и post–hoc анализ Тьюки. *Результаты и обсуждение.* Текстурный анализ мышечно–апоневротического слоя передней брюшной стенки выявил значимые различия между группами по Вейвлет- и Габор-анализу ($p < 0,0001$). Пациенты группы 2 существенно отличались от групп 1 и 3, тогда как группы 1 и 3 демонстрировали схожие характеристики тканей ($p > 0,05$), что может свидетельствовать об адаптационных изменениях у пациентов с наиболее выраженными грыжевыми дефектами. У пациентов группы 2 наблюдаются выраженные изменения структуры мышц, что подтверждается значимыми различиями по контрастности ($p < 0,0001$), корреляции ($p < 0,0001$) и куртозису ($p = 0,001$). При этом средняя яркость и однородность не показали статистически значимых различий между группами ($p > 0,05$), что указывает на схожесть общего распределения интенсивностей сигнала. Выводы. Наиболее выраженные признаки структурной дезорганизации мышечно-апоневротического слоя выявлены у пациентов с W2–ПОВГ, что указывает на морфофункциональную нестабильность. В группе W3–ПОВГ преобладают адаптационные процессы. Выявленные закономерности подтверждают этапность морфологических изменений при ПОВГ и подчеркивают значимость текстурного анализа для персонализированного хирургического планирования.

Ключевые слова: текстурный анализ, послеоперационная вентральная грыжа, мышечно-апоневротический слой, структурные изменения, адаптационные изменения, фиброз, хирургическая тактика.

Информация о финансировании: работа выполнена без финансовой поддержки.

Информация о конфликте интересов. Авторы заявляют об отсутствии конфликтов интересов.

Вклад авторов: А.В. Протасов, Л.Б. Канахина, О.И. Мазурова — концепция и дизайн исследования; О.И. Мазурова, А.В. Протасов — сбор и обработка материалов; Л.Б. Канахина, А.В. Протасов — анализ полученных данных, О.И. Мазурова, А.В. Протасов — написание текста и редактирование текста

Благодарности — неприменимо.

Информационное согласие на публикацию. Пациенты предоставили добровольное информированное согласие на обработку персональных данных и публикацию.

Поступила 11.04.2025. Принята 01.07.2025.

Для цитирования: *Protasov A.V., Kanakhina L.B., Mazurova O.I.* Musculoaponeurotic layer structural alterations of the anterior abdominal wall in ventral hernias: insights from CT texture analysis // Вестник Российского университета дружбы народов. Серия: Медицина. 2026. Т. 30. № 1. С. 80–91. doi: 10.22363/2313-0245-2026-30-1-80-91. EDN: CYTWAR

Corresponding author: Kanakhina Liya Beketaevna —Postgraduate Student at the Department of Operative Surgery and Clinical Anatomy named after I.D. Kirpatovsky, RUDN University, 117198, Miklukho-Maklaya str., 8, Moscow, Russian Federation. E-mail: glb.1994@mail.ru
Kanakhina L.B. ORCID 0000-0003-0260-1478
Protasov A.V. ORCID 0000-0001-5439-9262
Mazurova O.I. ORCID 0000-0003-2677-6272

Ответственный за переписку: Канахина Лия Бекетаевна, аспирант кафедры оперативной хирургии и клинической анатомии имени И.Д. Кирпатовского, Российский университет дружбы народов имени Патриса Лумумбы, 117198, г. Москва, ул. Миклухо-Маклая, д. 8. E-mail: glb.1994@mail.ru
Канахина Л.Б. SPIN 6555-8191, ORCID 0000-0002-9159-4232
Протасов А.В. SPIN 3126-7423, ORCID 0000-0001-5439-9262
Мазурова О.И. SPIN 6541-7112, ORCID 0000-0003-2677-6272